[11]N. Levinson, Kgl. Danske Videnskab. Selskab, Mat.-Fys. Medd. 25, No. 9 (1949).
[12]W. J. Swiatacki, Proc. Phys. Soc. (London) A64, 226 (1951).
[13]A. H. Kahn and H. P. R. Freiderikse, in *Solid State Physics*, edited by F. Steitz and D. Turnbull (Academic, New York, 1959), Vol. 9, p. 257.

PHYSICAL REVIEW B VOLUME 5, NUMBER 2 15 JANUARY 1972

# Interband Transitions and Exciton Effects in Semiconductors*

M. Welkowsky and R. Braunstein
*Department of Physics, University of California, Los Angeles, California* 90024
(Received 19 July 1971)

The band structures of Ge, Si, GaAs, GaP, GaSb, InAs, InP, InSb, and AlSb have been studied in reflectivity in the energy region 1.6–5.0 eV at temperatures ranging from 80 to 300 °K. Utilizing a double-beam, single-detector wavelength-modulation system, and ensuing Kramers-Krönig analyses, experimentally unambiguous line shapes have been obtained for the real and imaginary part of the dielectric constants, permitting the identification of the types of critical points involved in an optical transition, and the determination of the existence of hyperbolic exciton interactions. Such an interaction has been verified in all materials, except Si, as an $M_1$ critical point located at $\Lambda$ in the Brillouin zone. The location and energy of the interband transition in these semiconductors correlates with existing band calculations. The interband transitions in Si are dominated by structure from a large region of the Brillouin zone. The high-energy $E_2$ transitions in all materials give evidence of a multiplicity of critical-point structure.

## I. INTRODUCTION

The band structures of Ge, Si, GaAs, GaP, GaSb, InAs, InP, InSb, and AlSb have been studied in reflectivity in the energy region 1.6–5.0 eV at temperatures ranging from 80 to 300 °K. Utilizing a double-beam, single-detector wavelength-modulation system and ensuing Kramers-Krönig analyses, experimental line shapes have been obtained for the derivative of the real and imaginary parts of the dielectric constant. These analyses enable the identification of the types of critical points involved in the optical transition as well as the existence of hyperbolic exciton interactions.

Reflectivity derivative data using wavelength modulation[1] have been previously used to obtain interband transition energies of several of these semiconductors.[2–6] Shaklee *et al.*[2] observed the reflectance derivative spectra of InSb in the neighborhood of the $E_1$ and $E_1+\Delta_1$ structure; by studying the line shapes of the spectra, they obtained evidence for the contribution of exciton effects to the observed transitions. Evidence for the existence of hyperbolic excitons in GaAs by means of the polarization-dependent splitting of the $E_1$ and $E_1+\Delta_1$ structure was obtained by Rowe *et al.*[3] Wavelength-modulated reflectance measurements on the $InAs_{1-x}P_x$ alloys were studied by Thompson *et al.*[4] in the spectral region of the $E_1$ and $E_1+\Delta_1$ transitions. Zucca and Shen[5] observed the wavelength-modulation spectra of GaAs, GaSb, InAs, InSb, Ge, and Si and correlated the spectra with existing band calculations for these crystals. From the sharpening of the spectra with reduced temperature due to the reduction of lifetime broadening, it was indicated that hyperbolic excitions are associated with the $E_1$ peaks. Since Kramers-Krönig analyses were not performed on these reflectance data to obtain the derivative of $\epsilon_1$ and $\epsilon_2$, a direct comparison of line shapes with theory was not possible. Further evidence for excitonic effects on the $E_1$ and $E_1+\Delta_1$ transition in InAs was obtained by Antoci *et al.*[7] by studying the temperature dependence of the line shapes of the $E_1$ and $E_1+\Delta_1$ structure using thermoreflectance. The band structure features of Ge, Si, GaAs, GaSb, GaP, InAs, InSb, InP, and AlSb were studied by the present authors[6] in the spectral region 1.62–5.08 eV as a function of temperature using a double-beam single-detector wavelength-modulated reflectance system. Structures corresponding to various critical points were seen and related to existing band calculations. The above observations using wavelength-modulation techniques have all indicated that the reflectance spectrum in the $E_1$ region cannot be explained within the framework of the one-electron approximation with lifetime broadening corrections, and suggest that Coulomb interaction should be included to explain the observed structure. The prior work on these substances have involved either a number of substances in a restrictive spectral region or in most cases have reported only the derivative of the re-

flectance rather than the derivative of $\epsilon_1$ and $\epsilon_2$ which are quantities more amenable for comparison with theory. Although the shape of $R(\omega)$ and $\epsilon_2(\omega)$ or their respective derivatives are usually similar, the peaks in the respective representations are usually shifted with respect to each other by as much as 0.4 eV at higher energies. Despite the fact that $\epsilon_1$ and $\epsilon_2$ and their derivatives are related by the Kramers-Krönig transform, it is sometimes convenient to have both quantities available to elucidate observed structures with theory, especially so in cases where weak and strong singularities overlap in energy. Such analyses are presented in the present work for the region 1.6–5.08 eV, accompanied by line-shape analyses which enable the location and energies of the interband transitions in these semiconductors to be correlated with existing band calculations and corroborate the existence of exciton effects above the fundamental gap in these materials.

In order to achieve high sensitivity and accuracy in optical measurements of solids, several modulation techniques have been developed which employ conventional phase-sensitive detection methods to extract small spectral changes occurring in a relatively smooth, but large, background. There are essentially two different methods of obtaining the derivativelike spectra. One approach is the modulation of a material parameter,[8–14] such as the lattice constant, or a periodic change of some property of the crystal structure. This can be accomplished with electric fields, pressure, and temperature modulation. On the whole, the experimental situation is straightforward, but the resulting line shapes of the derivative spectra are quantitatively difficult to interpret; this is caused by the perturbation applied to the band structure by the experimental system.

The alternative approach is to leave the sample unchanged, and modulate a component of the external measuring system, such as the output of a monochromator. With this technique of wavelength modulation,[1,15,16] line shapes are obtained which can be related to the theory of the optical constants of a material. In order to identify the types of critical points involved in an optical transition and to determine whether exciton interactions exist, experimentally unambiguous line shapes are necessary. However, with this technique, as with all conventional reflectivity measurements, the existence of an intrinsic space charge layer on the surface can influence the observed structure.

## II. CRITICAL POINTS AND EXCITONS

From the one-electron model of optical absorption, the contribution to the dielectric constant of a material is large in the neighborhood of the critical-point energies, i.e., when the condition

$$|\nabla_{\vec{k}}(E_c - E_v)| = 0 \tag{1}$$

is fulfilled. $E_c$ is the conductance-band energy, $E_v$ is the valence-band energy, and $\vec{k}$ is the wavevector. It is at these points in the Brillouin zone that changes in the absorption occur.

In principle, exciton states should exist at each type of critical point, since the definition of a critical point [Eq. (1)] is identical with the condition that an excitonic interaction is most probable when the relative velocity between the electron and hole is smallest. However, above the fundamental edge, the theory of excitonic interactions at saddle points is complicated, due to the complexity of solving the Schrödinger equation with one or more negative masses, and a reasonably realistic potential.

Saddle-point excitons, or hyperbolic excitons (so named because the constant-energy surfaces around three-dimensional saddle points are hyperboloids) cause modifications to the one-electric line shapes of the dielectric constant. Several approaches have been tried in an attempt to explain the nature of hyperbolic excitions. Phillips[17] expanded upon a resonance scattering formalism[18] for atomic interactions to develop a phenomenological theory for semiconductors. Because of the large static dielectric constants of the diamond and zincblende semiconductors, the exciton binding energies are small; hence, any exciton effects are likely to be degenerate with the continuum of structure due to interband transitions. The results basically predict an asymmetry in the line shape of the imaginary part of the dielectric constant $\epsilon_2$ because of interference between the resonant discrete states and the continuous scattering background.

Many theories dealing with the nonhydrogenic hyperbolic excition problem approximate the interaction by truncating it beyond a given distance of the electron-hole separation $\vec{r}$. The most common method is the contact potential of the Koster-Slater interaction[19]

$$V(\vec{r}) = \delta(\vec{r})g \ , \tag{2}$$

where $g$ is a constant which gives the strength of the interaction; it is negative for attractive potentials. $V(\vec{r})$ is zero unless the electron and hole are on the same unit cell, a condition better suited to polar materials than to the III-V and group-IV semiconductors. Using this interaction, it has been found[20] that $\epsilon_2$ line shapes sharpen at $M_1$ critical points, but weaken at $M_2$ critical points.

Calculations[21] using a tight-binding model restricted to nearest neighbors have shown that an exciton at an $M_i$ critical point produces a line shape for $\epsilon_2$ which is an admixture of the line shapes for an $M_i$ and $M_{i+1}$ critical point ($M_4 \equiv M_0$). This holds

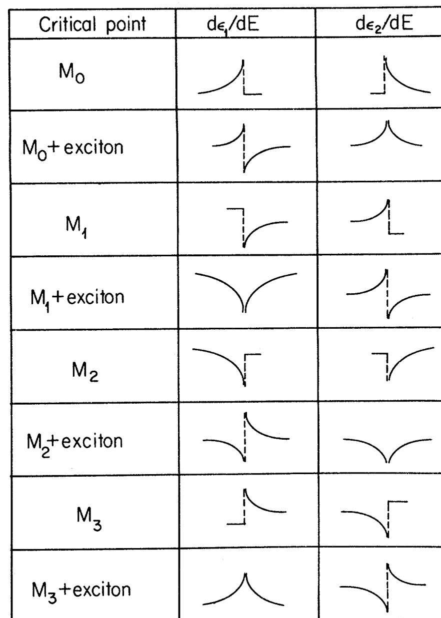


FIG. 1. Line shapes of the real and imaginary part of the dielectric constant at the various types of critical points, including exciton effects.

for the real part of the dielectric constant $\epsilon_1$ also. The derivatives of these line shapes with respect to energy are presented in Fig. 1. At each $M_i$ singularity, the one-electron line shapes are given. The effect of an exciton is shown for an equal admixture of the adjacent one electron line shapes. Kane[22] considered the effect of Coulomb interaction between electron and hole at an $M_1$ critical point in the effective-mass approximation using the adiabatic method.[20] Quantitative agreement was found for this calculation and the structure in $\epsilon_2$ for CdTe at 3.5 eV measured by Marple and Ehrenreich.[23] On the basis of this detailed agreement, Kane[22] indicated that it is likely that most of the line shapes of the column IV, III-V, and II-VI semiconductors can be explained in a similar manner.

The strongest criticism to be leveled against these methods of calculation in terms of their applicability to semiconductors is in reference to their use of a short-range interaction. A recent calculation[24] utilizing a resolvent formalism has shown that hyperbolic excitons occur for long range interactions. This calculation was performed for solid Xe, with a dielectric constant of 2.2. For the semiconductors under consideration, the dielectric constants are larger (~ 10–15), so that the electron-hole coupling is weaker. Strong support for the extension of this calculation to semiconductors comes from the fact that the predicted resonances remain significant at large electron-hole separations, the precise conditions that prevails in a semiconductor resonance. However, it must be noted that no detailed theories exist which are specifically concerned with the effects of the exciton interaction above the fundamental edge in semiconductors, and which incorporate realistic long-range interaction potentials.

It is possible for the above mentioned admixture of line shapes to occur without the existence of an exciton. The structure could be explained[23] as due to an appreciable nonparabolicity of the energy bands near a critical point, such as the accidental degeneracy of an $M_1$ and $M_2$ singularity. Current band calculations[25–27] do not recognize such an occurrence in the vicinity of the $E_1$ transitions[9] for the diamond and zincblende semiconductors; exciton effects must be considered.

An important factor in recognizing an excitonic interaction is the presence of an asymmetric line narrowing with decreasing temperature. As the temperature is lowered, the excitonic broadening, caused by phonons, is greatly reduced.

## III. EXPERIMENT

A double-beam, single-detector wavelength-modulation system was utilized, which allows shot-noise-limited measurements with a sensitivity of one part in $10^5$ at a time constant of 3 sec. This system has been described in detail elsewhere.[28] The wavelength modulation was obtained by oscillating the output diagonal mirror in a Perkin-Elmer 99G monochromator by means of an electromechanical drive. The depth of modulation was controllable up to a range of $\Delta\lambda/\lambda \sim 10^{-2}$; a modulation amplitude of 5–8 Å was used throughout these measurements with a resulting spectral resolution of ~ 0.003 eV. Quartz-iodine and xenon arc sources were used in the appropriate spectra regions. The single detector was an EMI 9558QB photomultiplier.

Reflectivity studies require careful preparation of the sample surface because the total effect takes place within the penetration depth of the light. Chemical etching was used to remove the final damaged layer from the hand-polished samples. Etching helps prevent extrinsic line broadening caused

TABLE I. Chemical etchants used for semiconductors.

| Sample | Etch | Time |
|---|---|---|
| Ge | $HF : HNO_3 : CH_3COOH$ (3:5:3) | 1 min |
| Si | $HF : HNO_3 : CH_3COOH$ (3:5:3) | 2 min |
| GaP | $HNO_3 : HCl$ (1:1) | 1 min |
| GaAs | $HNO_3 : HCl$ (1:1) | 30 sec |
| GaSb | $HF : HNO_3 : CH_3COOH$ (1:2:1) | 15 sec |
| InP | $HNO_3 : HCl$ (1:1) | 30 sec |
| InAs | $HNO_3 : HCl$ (1:1) | 1 min |
| InSb | $HF : HNO_3 : CH_3COOH$ (1:2:1) | 10 sec |
| AlSb | unetched | |

by the mechanical polishing and aids in cleaning the sample surface.

Table I lists the etchants used in this study. For the duration of the reaction, the chemical bath was slowly agitated so as to continuously present a fresh solution to the sample surface. To minimize surface oxidation when transferring the sample from the etching solution to the distilled-water rinse, the etchant was fully displaced by the rinsing solution, prior to the removal of the sample. The sample was then dried and immediately inserted into a Dewar, which was evacuated to $3\times10^{-6}$ Torr.

In all cases, the etch was found to be far more critical to the reproducibility of the reflectivity structure, rather than the quality of the final mechanical polish.

The values of $\epsilon_1$ and $\epsilon_2$ and their respective derivatives were all calculated with the aid of a Kramers-Krönig computer program, using the experimental derivative data $(1/R)dR/dE$. A compilation of this program has been given elsewhere.[29]

## IV. DISCUSSION OF RESULTS

The derivative reflectance spectra of the semiconductors studied, displayed in Figs. 2–10, were previously reported,[6] and are presented here for continuity of discussion. The derivatives of $\epsilon_1$ and $\epsilon_2$ (except for AlSb), obtained at 80 °K, are also shown in Figs. 2–10. The spectra show the characteristic groups of transitions which have become a familiar landmark for these materials, indicating the similarity in their band structure. The general groupings of these features are indicated in the respective figures, using the conventional notation.[9] Along with the dominant structures whose derivatives go through zero, indicating peaks in the reflectivity, a number of partially resolved peaks are seen.

Since peaks in the normal reflectivity spectra are usually designated as the position of a transition, the following procedure has been used to determine the energy of a transition from the experimental derivative curves. A zero crossing, from positive to negative, yields a reflectivity peak. An inflection point in the reflectivity spectra is indicated by a nonzero, positive or negative, minimum in the derivative. Table II lists the energies of the observed transitions, along with the assignments made as to their location in the Brillouin zone.

Since energy-band theories usually calculate optical transitions in terms of $\epsilon_2$, the Kramers-Krönig program has been used to obtain the experimental $\epsilon_2$ values. The transition energies obtained from the $\epsilon_2$ curves are also listed in Table II, and represent maximums or inflection points in $\epsilon_2$. The "local" character of the Kramers-Krönig analysis, relating a maximum in $\epsilon_2$ to a negative maximum in the slope of $\epsilon_1$, has been used to determine the

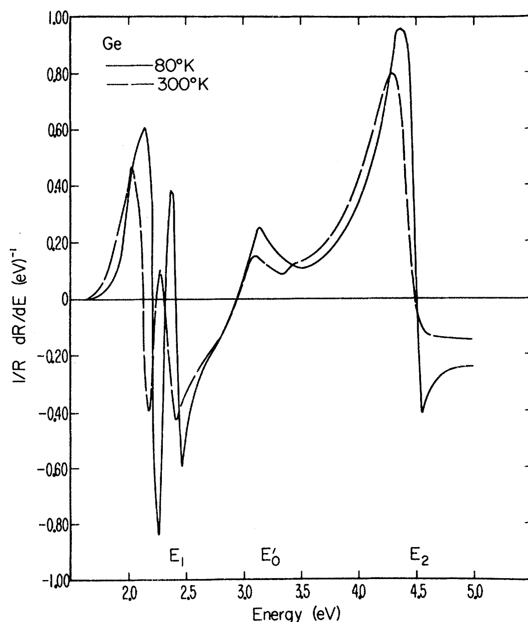


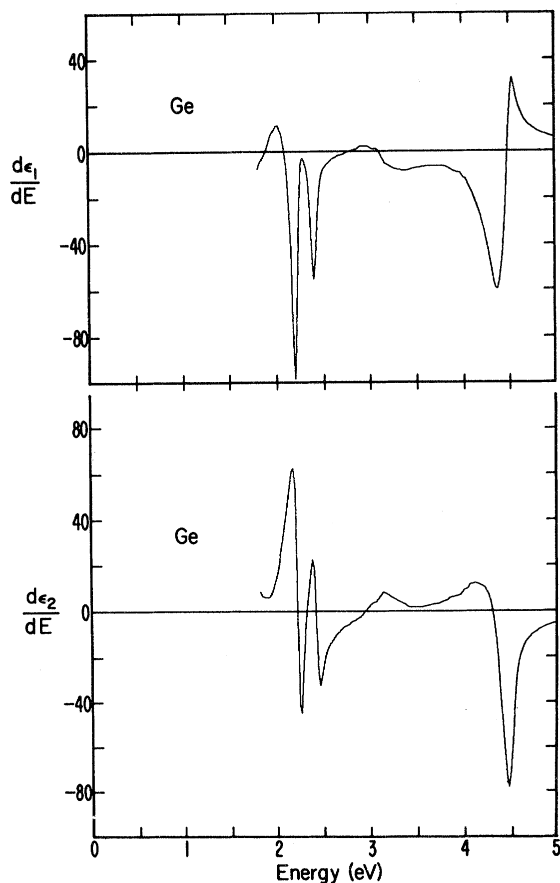


FIG. 2. Experimentally determined logarithmic derivative reflectivity spectra of Ge at 80 and 300 °K are shown in the top curves. Derivatives of $\epsilon_1$ and $\epsilon_2$ of Ge at 80 °K as calculated from the above data by the Kramers-Krönig transform are shown in the lower curves.

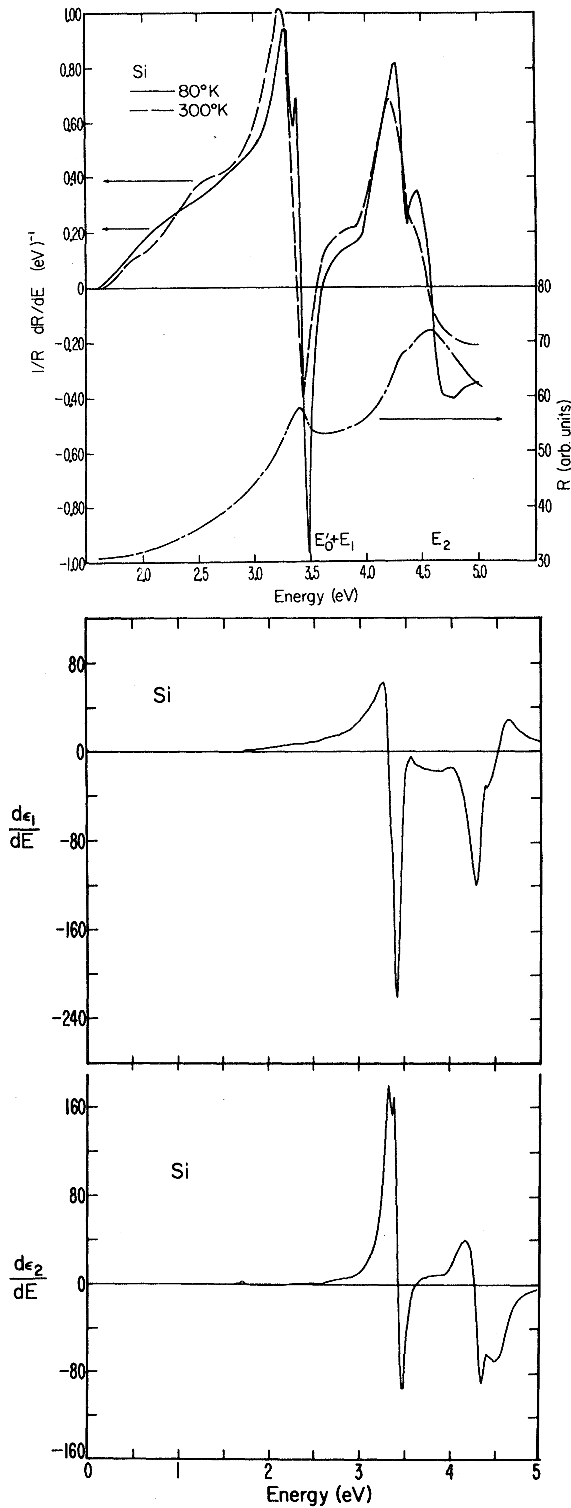


FIG. 3. Experimentally determined logarithmic derivative spectra of the reflectivity of Si at 80 and 300 °K and the normal reflectivity spectrum at 80 °K are shown in the top curves. Derivatives of $\epsilon_1$ and $\epsilon_2$ of Si at 80 °K as calculated from the above data by the Kramers-Krönig transform are shown in the lower curves.

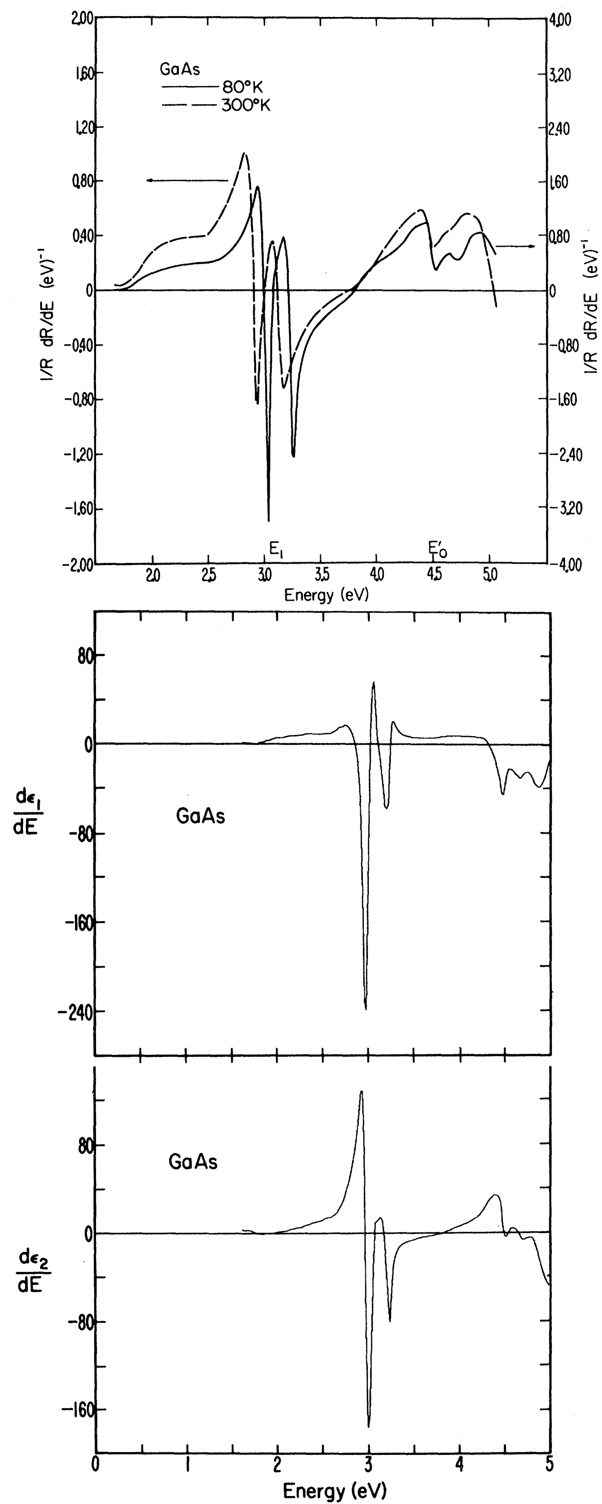


FIG. 4. Experimentally determined logarithmic derivative reflectivity spectra of GaAs at 80 and 300 °K are shown in the top curves. Derivatives of $\epsilon_1$ and $\epsilon_2$ of GaAs at 80 °K as calculated from the above data by the Kramers-Krönig transform are shown in the lower curves.

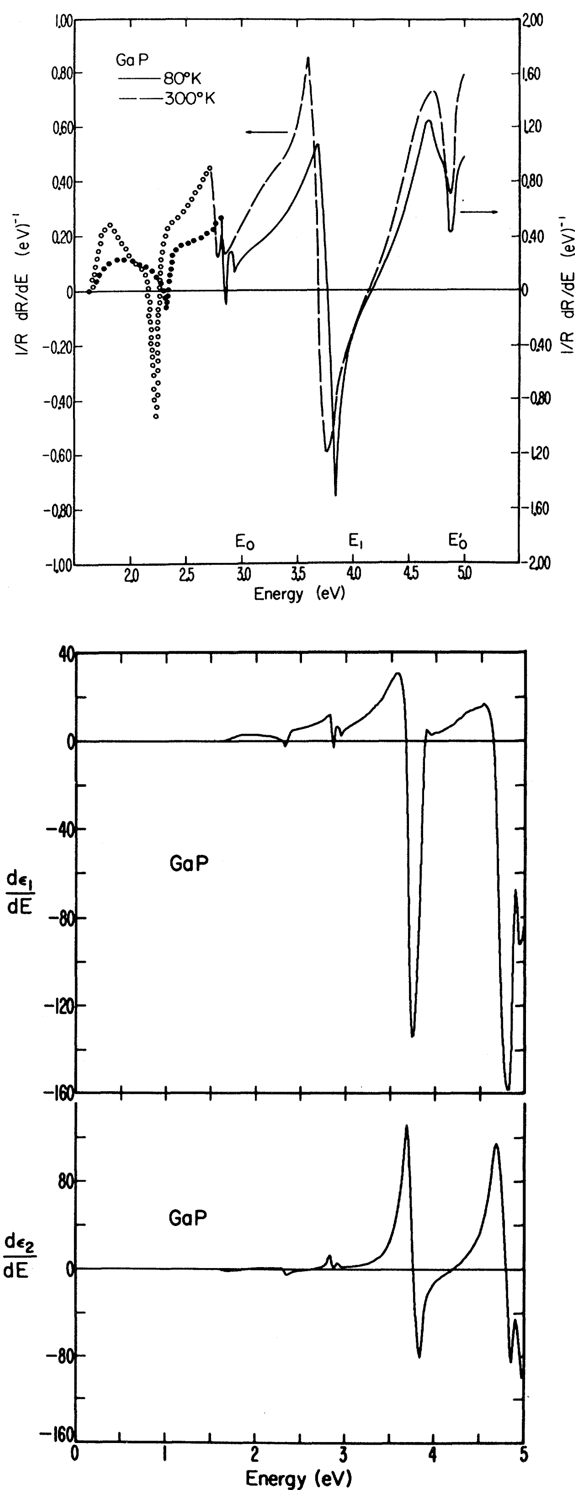


FIG. 5. Experimentally determined logarithmic derivative reflectivity spectra of GaP at 80 and 300°K are shown in the top curves. Dotted portion is the region where the sample is transparent. Derivatives of $\epsilon_1$ and $\epsilon_2$ of GaP at 80°K as calculated from the above data by the Kramers-Krönig transform are shown in the lower curves.

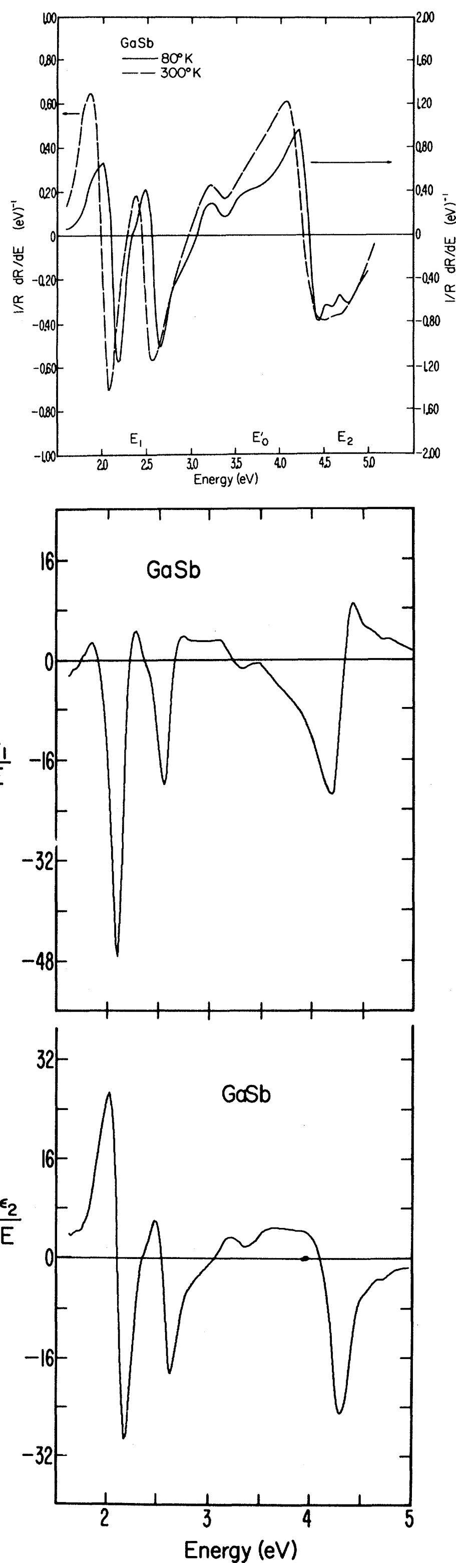


FIG. 6. Experimentally determined logarithmic derivative reflectivity spectra of GaSb at 80 and 300°K are shown in the top curves. Derivatives of $\epsilon_1$ and $\epsilon_2$ of GaSb at 80°K as calculated from the above data by the Kramers-Krönig transform are shown in the lower curves.

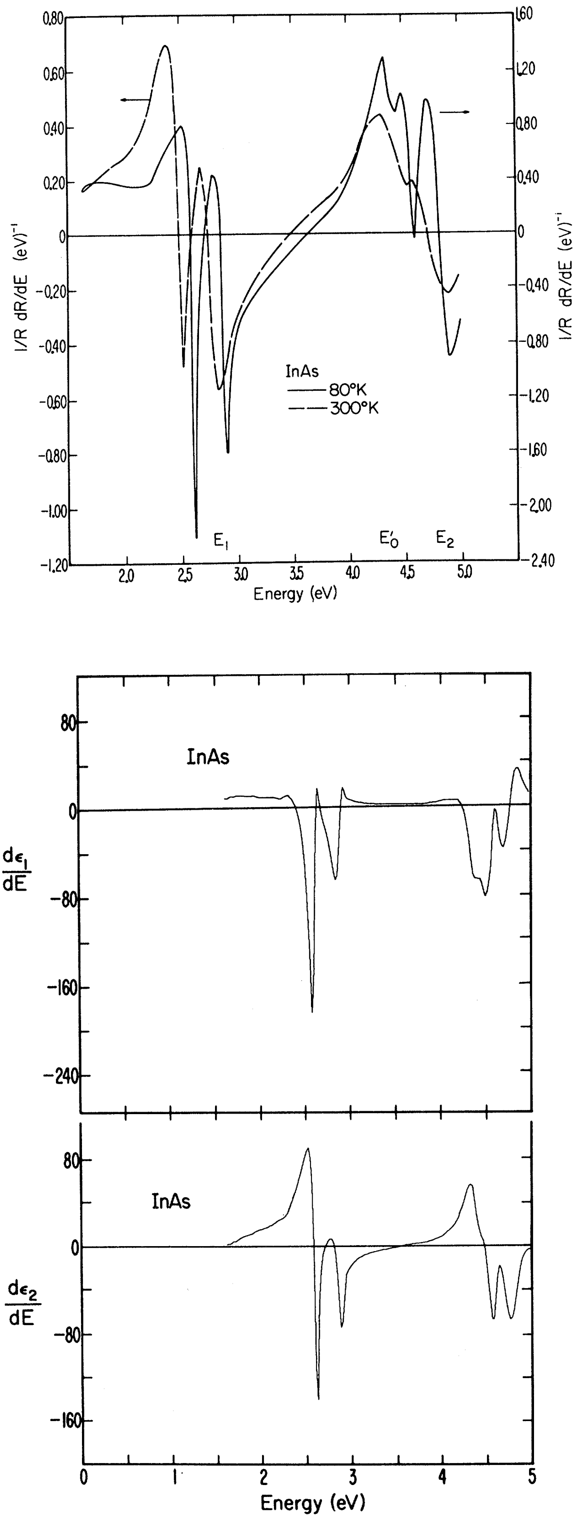


FIG. 7. Experimentally determined logarithmic derivative reflectivity spectra of InAs at 80 and 300 °K are shown in the top curves. Derivatives of $\epsilon_1$ and $\epsilon_2$ of InAs at 80 °K as calculated from the above data by the Kramers-Krönig transform are shown in the lower curves.

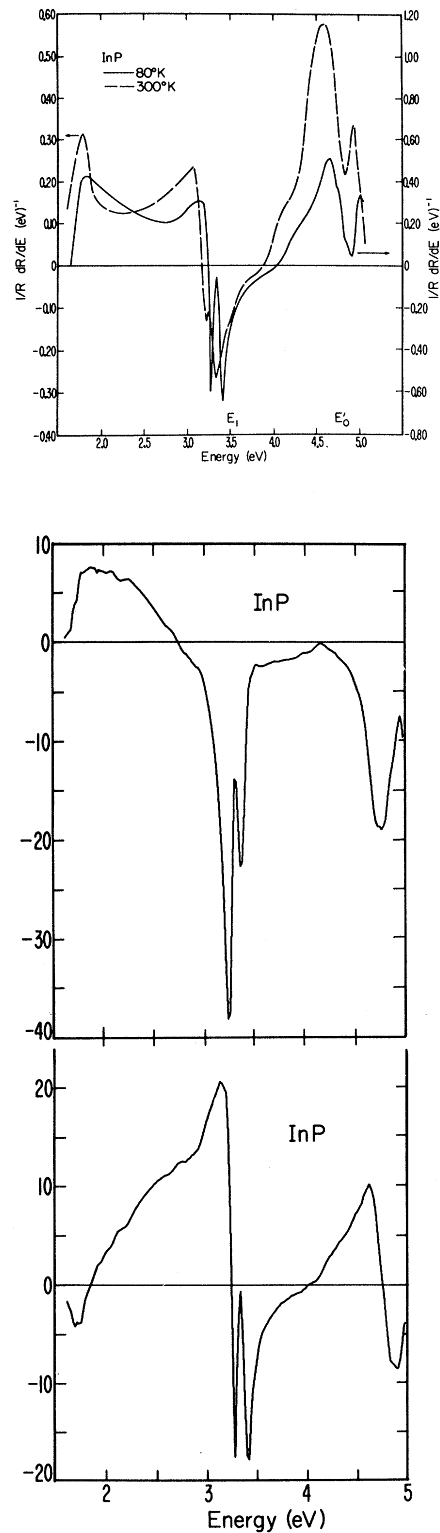


FIG. 8. Experimentally determined logarithmic derivative reflectivity spectra of InP at 80 and 300 °K are shown in the top curves. Derivatives of $\epsilon_1$ and $\epsilon_2$ of InP at 80 °K as calculated from the above data by the Kramers-Krönig transform are shown in the lower curves.

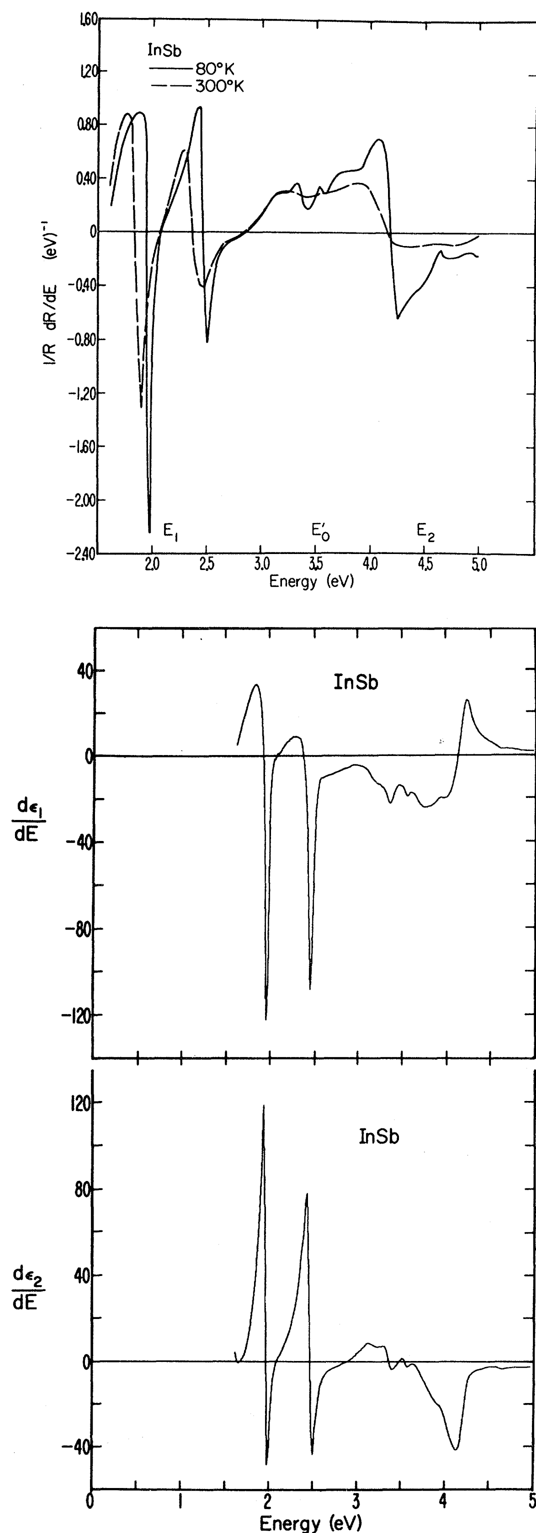


FIG. 9. Experimentally determined logarithmic derivative reflectivity spectra of InSb at 80 and 300 °K are shown in the top curves. Derivatives of $\epsilon_1$ and $\epsilon_2$ of InSb at 80 °K as calculated from the above data by the Kramers-Krönig transform are shown in the lower curves.

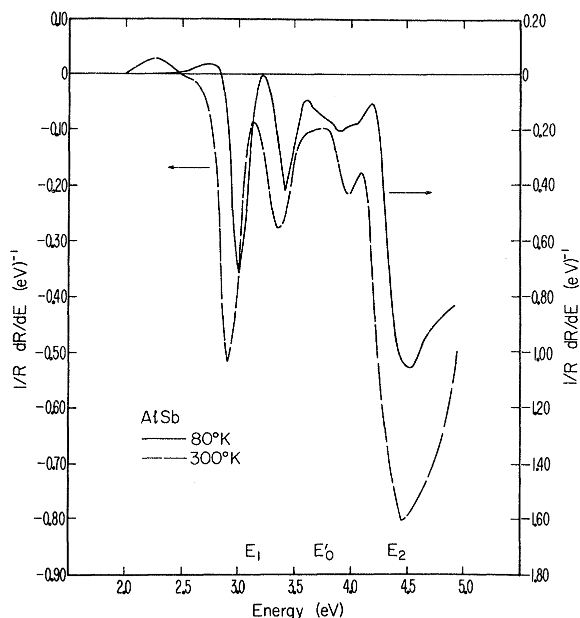


FIG. 10. Experimentally determined derivative spectra of the reflectivity of AlSb at 80 and 300 °K.

position of these inflection points. Also, the second derivative of $\epsilon_2$ has been calculated numerically from the experimentally determined first derivative, yielding the maximum curvature in $\epsilon_2$ in the vicinity of an inflection point. These two methods for finding the position of an inflection point have been found to correlate with each other. Additional information is produced by the second derivative. If one considers the case of a small peak superimposed on a large background, under the assumption that the curvature of $\epsilon_2$ due to the background is constant in the vicinity of the small peak, then one should observe a maximum in curvature at the energy of the small peak.

A comparison of the transition energies derived from the reflectivity derivative data and the $\epsilon_2$ analyses, listed in Table II, reveal the nonequivalence of the two, especially at high energies. Although the shapes of $R(\omega)$ and $\epsilon_2(\omega)$ are similar, the peaks are usually shifted[26] by as much as 0.4 eV for the transitions which occur with energy gaps near 5 eV. Because $\epsilon_2$ is derived from an integral transform of the reflectivity, fine structure in $\epsilon_2$ may be obscured. In this study, the Kramers-Krönig transform and ensuing analyses reproduced all peaks seen in $R(\omega)$, except for one transition in InSb, and one in GaSb.

As it is the line shapes of the dielectric constant that are of interest, the derivatives of these line shapes should be examined. The effects of excitons on these line shapes are subtle enough to require the sensitivity of wavelength-modulation analyses

TABLE II. Assignment of interband transitions in semiconductors. For each material, the interband transition energies as obtained from the reflectivity derivative data are given directly above the energies obtained from the $\epsilon_2$ data analysis. All values are from the 80 °K data unless otherwise noted. For AlSb, only reflectivity values are given. All energies are in eV.

| Sample | $\Lambda_3 \to \Lambda_1$ | $\Gamma_{25'} \to \Gamma_{15}$ | $\Gamma_{25'} \to \Gamma_{15}$ and $\Lambda_5 \to \Lambda_1$ (near $\Gamma$) | $\Delta_5 \to \Delta_1$ | $X_4 \to X_1$ | $\Sigma_2 \to \Sigma_3$ | $\Delta_5 \to \Delta_1$ (near $X$) |
|---|---|---|---|---|---|---|---|
| Ge | 2.212 2.420<br>2.219 2.416 | | 3.38<br>3.19 3.38 | | | 4.51<br>4.31 | |
| Si | | 3.36<br>3.34 | | 3.41<br>3.42 | ···<br>3.88 | 4.58<br>4.26 | 4.38<br>4.46 |

| Sample | $\Lambda_3 \to \Lambda_1$ | $\Gamma_{15} \to \Gamma_{15}$ and $\Delta_5 \to \Delta_1$ (near $\Gamma$) | $\Gamma_{15} \to \Gamma_{15}$ | $\Delta_5 \leftarrow \Delta_1$ | $\Sigma_2 \to \Sigma_3$ and $X_5 \to X_1$ | $\Delta_5 \to \Delta_1$ and $X_5 \to X_1$ | $\Delta_5 \to \Delta_3$ |
|---|---|---|---|---|---|---|---|
| GaAs | 2.981 3.211<br>2.971 3.178 | 4.52 4.72<br>4.50 4.67 | | | 5.04 ← (300 °K)<br>4.89 | | |
| GaP | 3.76<br>3.76 | | | | | 4.82 4.88<br>4.80 4.90 | |
| GaSb | 2.100 2.565<br>2.095 2.533 | | ··· ···<br>3.85 4.10 | 3.37 3.65<br>3.31 3.70 | 4.34 4.70<br>4.22 4.68 | | 4.52<br>··· |
| InAs | 2.588 2.859<br>2.580 2.804 | | | 4.44 4.60<br>4.37 4.47 | 4.82<br>4.70 | | |
| InP | 3.24 3.34<br>3.25 3.37 | | | 4.92 ···<br>4.70 4.78 | 5.07 ← (300 °K)<br>4.99 | | |
| InSb | 1.952 2.467<br>1.972 2.470 | | 3.42 3.79<br>3.36 3.74 | 3.22 3.58<br>3.18 3.56 | 4.20 4.66<br>4.04 4.64 | | 4.46 4.90<br>··· 4.84 |
| AlSb | 2.85 3.23 | 3.62 4.00 | | | 4.20 | | |
| | ±0.003 | ±0.02 | ±0.01 | ±0.01 | ±0.02 | ±0.02 | ±0.02 |

in order to recognize them. By comparing the line shapes of Figs. 2–10 to those of Fig. 1, while simultaneously taking into account the temperature dependence of the line shapes, as seen in Figs. 2–10, one can determine the possible existence of exciton effects above the fundamental edge. Furthermore, independent of exciton interactions, one can study the types of singularities responsible for a given optical transition.

In order to investigate the possibility that surface fields in the semiconductors may perturb the resulting line shapes of the wavelength-modulation data, the following procedure was used: A conventional electrolytic cell[9] was constructed, permitting wavelength-modulation reflectivity measurements to be performed on a Ge sample, with an applied dc voltage of 1 V across the cell's electrodes. This corresponds to a surface field of approximately $10^4$ V/cm. The line shapes obtained with or without the applied field were identical to within the sensitivity of the measuring system, negating a dependence of the wavelength-modulation spectra on the surface fields in these materials.

A hyperbolic exciton interaction in the vicinity of an $M_1$ critical point, specifically $\Lambda$, is a feature of the spectra of all the semiconductors in this study, save Si. As an example of a typical analysis, reference can be made to the Ge data of Fig. 2. It should be noted that the $d\epsilon_1/dE$ curve of the doublet near 2 eV has predominantly negative peaks with an abrupt high-energy side, while the $d\epsilon_2/dE$ curve is essentially symmetric about zero. The $\epsilon_1$ and $E_1 + \Delta_1$ doublet is generally associated with optical transitions at $\Lambda$ where band calculations[25,26] yield an $M_1$ critical point. From Fig. 1, we note that these shapes are similar to those due to an admixture of an $M_1$ and an $M_2$ singularity. From an examination of Fig. 2, a pronounced sharpening of the $E_1$ structure at 80 °K is evident; such line narrowing has been taken as evidence that exciton effects could play a role in the vicinity of the $M_1$ critical point.[2] In addition, present band-structure information[30] precludes the possibility of any accidental degeneracy of an $M_1$ and $M_2$ singularity in this region. Therefore, following the theoretical predictions[21,22] that such an admixture of $M_1$ and $M_2$ line shapes should result from a hyperbolic exciton interaction, the conclusion is that such an interaction does exist. Other experimental evidence has suggested the existence of the hyperbolic

exciton interaction in InSb[2] and in InAs.[6]

### A. Germanium

The distinct doublet at 2.219 and 2.416 eV are the $E_1$ and $E_1+\Delta_1$ transitions at $\Lambda(M_1)$, modified by exciton interaction, as described above. This sharp doublet characterizes the spectra of most of the semiconductors studied. No indication of any transitions associated with $L_{3'}\rightarrow L_1$, similar to the $e_1$ peaks observed by Potter,[31] has been obtained.

The $E_0'$ region is of particular interest in Ge. Band theory[30] shows that the greatest variation of any state as a function of the band model used is the $\Gamma_{15}$ state. Although only a shoulder is seen in the reflectivity derivative, the Kramers-Krönig analysis yields a doublet in $\epsilon_2$ at 3.19 and 3.38 eV. (It should be noted that this is the only case in this work where structure observed in reflection is enhanced by the Kramers-Krönig transform.) This is similar to structure seen in electroreflectance.[27] The $\Delta_0'$ splitting of 0.19 eV is less than the $\Delta_1$ splitting of 0.20 eV. A detailed analysis of the contributions from various pairs of valence and conduction bands in an empirical pseudopotential calculation[30] has shown that $\Gamma_{25'}\rightarrow\Gamma_{15}$ transitions are responsible for this doublet. Recent calculations[25,32] indicate that $\Delta_5\rightarrow\Delta_1$ transitions should be considered because of density-of-states arguments. However, the spin-orbit splitting at $\Delta$ would not be resolved in Ge.[33] The line shape in both $\epsilon_1'$ and $\epsilon_2'$ (the prime denotes differentiation with respect to energy) in this region suggests an admixture of $M_0$ and $M_1$ critical points. Therefore, the experimental results indicate that $\Gamma_{25'}\rightarrow\Gamma_{15}(M_0)$ and its spin-orbit split component are responsible for this structure, a conclusion which is supported by photoemission and transverse electroreflectance data[34]; this work and the present work yield a splitting of the conduction band at $\Gamma$ of 0.19 eV. A possibility exists that $\Delta_5\rightarrow\Delta_1$ transitions in the neighborhood of $\Gamma$ are accidentally degenerate. This would explain the contribution of an $M_1$ singularity.

The peak at 4.31 eV in $\epsilon_2$ is assigned to a degeneracy of an $M_1$ and an $M_2$ critical point. Exciton interaction in this region is ruled out because of an insufficient temperature dependence of this $E_2$ peak. The $\epsilon_2'$ line shape indicates that the $M_2$ critical point is strongly predominant. The $E_2$ peak is mainly associated with $\Sigma_2\rightarrow\Sigma_3(M_2)$ transitions, along the [110] symmetry axis. The large magnitude of this peak suggests that a large region of the Brillouin zone may be contributing to this transition. This is reinforced by the fact that a peak in $\epsilon_2$ must be due to a combination of singularities, if only interband transitions are considered. Volume effects in the vicinity of, but not at, $X(M_1)$,[33] degenerate with the $\Sigma$ transition above, would satisfy all singularity requirements.

### B. Silicon

The 3.4-eV peak in Si has been the subject of several papers,[30,33] and remains quite speculative. It has been shown[35,36] that the origin of this peak, and the associated structure resolved at 80 °K, is quite sensitive to the band model employed. Theory relates structure in this region to transitions at $\Gamma$, $L$, $\Lambda$, and $\Delta$, with emphasis on one or more of these depending on the particular calculation. The relative positions of $L$, $\Gamma$, and $X$ influence[33] the resulting line shapes of the critical point, and change the critical point energy.

The major peak in $\epsilon_2$ at 3.42 eV gives evidence of a multiplicity of critical points. The $\epsilon_1'$ curve yields a mixture of an $M_0$ and $M_1$ critical point, predominantly $M_1$ in nature due to the extent of the negative peak. The $\epsilon_2'$ curve shows the existence of an $M_1$ and an $M_2$ singularity, again mostly $M_1$ in character because of the strength of the positive peak. This is an example of a weak singularity in the presence of a strong singularity being more readily identified with the derivative of $\epsilon_1$ or $\epsilon_2$ as noted above. This suggests that the 3.42-eV peak is an $M_1$ singularity, and that the $M_0$ contribution may be due to the nearly degenerate 3.34-eV structure. Other transitions of nearly degenerate energy should also be considered to account for the diverse line shapes in this area. Exciton interaction is ruled out as there is not an admixture of the same adjacent singularities in both $\epsilon_1'$ and $\epsilon_2'$. Because the predominant peak at 3.42 eV is of $M_1$ character, it should be associated with either $\Lambda_3\rightarrow\Lambda_1$ or $\Delta_5\rightarrow\Delta_1$ transitions. It certainly is not due to $L_{3'}\rightarrow L_1$, which is $M_0$ in nature. The $\Lambda_3\rightarrow\Lambda_1$ transition is partially degenerate with $\Delta_5\rightarrow\Delta_1$ transition near $\Gamma$. Piezo-reflectance data[11] and band theory[35,36] suggest the $\Delta$ assignment.

A study of the room-temperature derivative reflectivity spectra of Ge-Si alloy was undertaken in order to observe the $E_1$ peak as a function of alloy concentration. The results are summarized in Fig. 11. The break in the curve at approximately 78 at.% Si may be taken to indicate that the $\Lambda$ transition, which is responsible for the $E_1$ peak in Ge, is no longer the origin for the Si transition.

With the $\Delta_5\rightarrow\Delta_1$ transition accounting for the $M_1$ singularity, the $M_0$ critical point is associated with $\Gamma_{25'}\rightarrow\Gamma_{15}$, responsible for the 3.34-eV structure, in agreement with band theory.[33] The $M_2$ character of the 3.42-eV peak is explained by the aforementioned degeneracy of $\Lambda$ and $\Delta$. That $\Lambda$ should have an $M_2$ singularity in this region has been shown.[33]

The very weak feature at 3.88 eV can be correlated with transitions in the region of $X$. Band calculations[30,36] predict a weak $X_4\rightarrow X_1$ contribution, but at slightly higher energy.

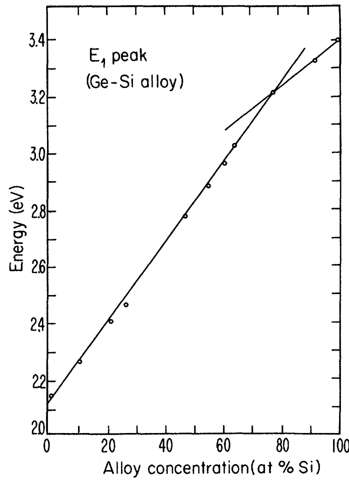


FIG. 11. $E_1$ peak of Ge-Si alloy as a function of alloy concentration, as measured by the zero crossing of the reflectivity derivative.

The $E_2$ regime has been studied in great detail,[37] with the finding that a multiplicity of critical points of low symmetry throughout the Brillouin zone, can be responsible for the large $E_2$ peak. This study shows that $M_1$ and $M_2$ singularities are involved; there is no temperature dependence to suggest the presence of excitons. The major contribution is associated with $\Sigma_2 \rightarrow \Sigma_3(M_2)$, and is identified with the 4.26-eV peak. The smaller structure at 4.46 eV is assigned to $\Delta_5 \rightarrow \Delta_1(M_1)$, near $X$. Volume effects seem to be occurring over a wide energy range, creating the degeneracies necessary to produce the peak at 4.26 eV.

### C. Gallium Arsenide

The $E_1$ transition at 2.971 eV is another example of an $M_1$ singularity plus a hyperbolic exciton. The sharpening of the derivative structure as the temperature is lowered (see Fig. 4) indicates the presence of the exciton. The spin-orbit split component at 3.178 eV follows the same pattern, taking into account the perturbation on its line shape caused by its neighbor, $E_1$. The doublet is assigned to $\Delta_3 \rightarrow \Delta_1(M_1)$.

The structure near 4.5 eV appears to be $M_1$-like from the $\epsilon_1'$ data, but $M_0$ and $M_1$ contribute to $\epsilon_2'$. The $M_1$ predominance corresponds to the predicted[25] $\Delta_5 \rightarrow \Delta_1$ transition. To account for the $M_0$ character of this peak, it is suggested that transitions at $\Gamma$ also be considered. In particular, photoemission data[38] have identified the $\Gamma_{15} \rightarrow \Gamma_{15}$ transition at 4.52 eV. In the III-V compounds, $\Delta$ is spin-orbit split, and this splitting gives rise to the 4.67-eV structure, also $M_1$ in nature.

There is a hint of an $M_2$ singularity in $\epsilon_1'$ near 4.9 eV. Unfortunately, the spectral range is limited so that the $\epsilon_2'$ line shape was not completely observed. If one assumes that the curve would gradually fall back to zero at higher energy, then this too would exhibit $M_2$ character. Consequently, the large peak at 4.89 eV in $\epsilon_2$ is caused almost entirely by $\Sigma_2 \rightarrow \Sigma_3(M_2)$.

### D. Gallium Phosphide

The structure below 3 eV, shown in Fig. 5 is due to indirect and fundamental direct gap transitions. The feature at 3.76 eV is strongly temperature dependent and is an $M_1$ singularity located at $\Lambda$ in the presence of an exciton. The structure at 4.80 eV is $M_0$ plus $M_1$ in nature, with a slight emphasis on $M_1$ from the $\epsilon_1'$ curve. This may be a result of the small 4.90-eV structure, which gives the appearance of an $M_1$ critical point in the $\epsilon_1'$ curve. This composite character is explained with a good fit to pseudopotential theory[25] as due to $\Delta_5 \rightarrow \Delta_1(M_0)$ and $X_5 \rightarrow X_1(M_1)$. The theoretical values are slightly lower in energy.

### E. Gallium Antimonide

Before discussing the results for GaSb, a word of caution is advanced. No optical reflectivity measurements could be found in the literature for GaSb above 5 eV. Thus, the high-energy extrapolation in the Kramers-Krönig analysis began at 5 eV, the last point of the derivative spectrum. This undoubtedly had some effect on the resulting line shapes; a test with other materials, removing the high energy data above 5 eV and extrapolating as in the GaSb case, did not always produce much change in the line shapes or transition energies.

The $E_1$ and $E_1 + \Delta_1$ doublet at 2.095 and 2.533 eV originate at $\Lambda$, the result of an $M_1$ singularity and a hyperbolic exciton. Identification of the character of the singularities causing the small structure between 3 and 4 eV could not be made because of the unresolved nature of the line shapes; recourse to band theory must be made. An excellent fit with theory[32] is achieved by correlating the spin-orbit splittings along $\Delta$ and $\Gamma_{15}^c$. The theoretical splitting for the valence band at $\Delta$ is 0.35 eV, compared to the 0.39-eV value between the experimental 3.31- and 3.70-eV transitions. The calculated splitting of the conduction band at $\Gamma_{15}$ is 0.24 eV, compared to the experimental value of 0.25 eV between the 3.85- and 4.10-eV transitions. Thus, the 3.31-eV transition is assigned to $\Delta_5 \rightarrow \Delta_1$ with the 3.70-eV transition being its spin-orbit component. The structures at 3.85 and 4.10 eV are assigned to transitions from the top valence band $\Gamma_8$ to the split upper conduction band $\Gamma_{15}(\Gamma_7$ and $\Gamma_8)$.

The high-energy peaks above 4.2 eV are associated with a combination of $M_2$ and $M_3$ critical points. The $\Sigma_2 \rightarrow \Sigma_3(M_2)$ transition must be considered on the basis of the line shape analysis, al-

though the splitting of 0.46 eV is a reasonably good fit to the expected splitting at $X(M_0)$. A recent calculation[39] has determined that transitions at $X$ ($X_5 \rightarrow X_1$) also contribute to this structure, in addition to those at $\Sigma$. A transition at 4.52 eV in the reflectivity derivative data was not observed in $\epsilon_2$. This feature may be indicative of $\Delta_5 \rightarrow \Delta_3$, by comparison to the InSb results.

### F. Indium Arsenide

The common feature of an exciton effect at $\Lambda$ is again found, at the 2.580- and 2.804-eV peaks. The split transition at 4.37 and 4.47 eV is assigned to $\Delta_5 \rightarrow \Delta_1(M_1)$. The strong increase in magnitude of the 4.7-eV peak with a decrease in temperature, noted in other modulation data,[5] coupled with the line shapes of $\epsilon_1'$ and $\epsilon_2'$, suggest that this peak is due to an $M_2$ singularity accompanied by an exciton. The transition is associated with $\Sigma_2 \rightarrow \Sigma_3$.

### G. Indium Phosphide

The 3.25- and 3.37-eV doublet displays the characteristics of the exciton-$M_1$ interaction, and is associated with $\Lambda_3 \rightarrow \Lambda_1$. The 4.7-eV peak would appear to be due to an $M_1$ plus $M_2$ mixture. It and its spin-orbit split component at 4.80 eV are assigned to $\Delta_5 \rightarrow \Delta_1(M_1)$ transitions near $\Gamma$. The transition at 4.99 eV revealed itself as a peak in the density of states function of the Kramers-Krönig analysis, and was not observed in $\epsilon_2$. The density-of-states calculation assumed constant-momentum matrix elements. This peak is associated with $\Sigma_2 \rightarrow \Sigma_3$, although transitions at $X$ may also occur. (This peak was seen at 5.07 eV at 300 °K in the reflectivity derivative data.)

### H. Indium Antimonide

The line narrowing of the $E_1$ doublet is more evident in InSb than in any other semiconductor studied. This suggests that an $M_1$ critical point with a hyperbolic exciton is responsible for the observed line shapes. The transitions at 1.972 and 2.470 eV originate at $\Lambda$.

The multitude of structure in the 3.5 eV region is quite small, but there is a hint of $M_1$ and $M_2$ singularities; the structure can be determined by comparing spin-orbit splittings to theory.[40] Both experimental splittings are 0.38 eV, while that predicted for $\Delta_0'$ (at $\Delta$ in the Brillouin zone) is 0.42 eV and the $\Delta_{15}$ splitting of the upper conduction band is 0.38 eV. As in the case of GaSb, the first pair of transitions (3.18 and 3.56 eV) are assigned to $\Delta_5 \rightarrow \Delta_1(M_1)$, and the second pair of transitions (3.36 and 3.74 eV) are associated with $\Gamma_{15} \rightarrow \Gamma_{15}$.

The 4.04-eV peak in $\epsilon_2$ is associated with an admixture of $M_2$ and $M_3$ critical points, and is assigned to $\Sigma_2 \rightarrow \Sigma_3(M_2)$, degenerate with a transition at $X(X_5 \rightarrow X_1)$. The splitting between this peak and that at 4.64 eV is commensurate with the $X_3 \rightarrow X_1$ splitting in the conduction band. The small structure at 4.84 eV is believed to be due to $\Delta_5 \rightarrow \Delta_3$. A spin-split pair in the reflectivity derivative spectrum, at 4.46 and 4.90 eV, is the $\Delta_5 \rightarrow \Delta_3$ spin-orbit split transition. The lower-energy component has been obscured by the Kramers-Krönig transform.

The similarity in the band structure of GaSb and InSb is evident. This is made even more apparent by the line-shape analysis which predicts an $M_3$ singularity at the high-energy transitions in both materials. In neither case can such an assignment be made at this time.

### I. Aluminum Antimonide

As seen in Fig. 10, the derivative of the reflectivity of AlSb is always negative; hence, the reflectivity is constantly dropping. This result was most probably caused by the adsorption of water onto the surface of the hydroscopic material. A similar reflectivity spectrum has been previously reported.[41] However, preparing the sample by cleaving under ultrahigh vacuum produced[42] the "normal" reflectivity spectrum expected from a III-V compound. Because of this suspect character of the reflectivity spectrum, no line-shape analysis was attempted.

Based on the reflectivity data, the line narrowing with a decrease in temperature for the transitions at 2.85 and 3.23 eV indicates the presence of an exciton at $\Lambda$. The structure at 3.62 and 4.00 eV is tentatively assigned to either $\Gamma_{15} \rightarrow \Gamma_{15}$ or $\Delta_5 \rightarrow \Delta_1$ transitions. The 4.20-eV peak is tentatively assigned to either $\Sigma_2 \rightarrow \Sigma_3$ or $X_5 \rightarrow X_1$. These assignments await a line-shape analysis on $\epsilon_1$ and $\epsilon_2$ for confirmation, on a properly prepared sample.

TABLE III. Spin-orbit splittings. The $\Delta_1$ and $\Delta_0'$ calculated values are from Refs. 27 and 43. The $\Delta_0$ calculated values are from Ref. 26. All values taken from $\epsilon_2$ data except for AlSb, which is taken from reflectivity derivative data. All energies are in eV.

| | $\Delta_1$ | | $\Delta_0'$ | | $\Delta_0$ |
|---|---|---|---|---|---|
| Sample | Expt. | Calc. | Expt. | Calc. | Calc. |
| Ge | 0.20 | 0.20 | 0.19 | 0.17 | 0.29 |
| Si | ... | 0.03 | ... | ... | 0.04 |
| GaAs | 0.21 | 0.22 | 0.17 | 0.17 | 0.35 |
| GaP | ... | 0.07 | 0.10 | 0.07 | 0.13 |
| GaSb | 0.44 | 0.46 | 0.39 | 0.35[a] | 0.80 |
| InAs | 0.22 | 0.28 | 0.10 | 0.22 | 0.41 |
| InP | 0.12 | 0.11 | 0.08 | 0.08 | ... |
| InSb | 0.50 | 0.48 | 0.38 | 0.42[b] | 0.90 |
| AlSb | 0.38 | 0.41 | 0.38 | 0.47 | 0.75 |

[a]From Ref. 32. [b]From Ref. 40.

### J. Spin-Orbit Splittings

Table III summarizes the spin-orbit splittings at 80 °K, obtained from the $\epsilon_2$ data, compared to the theoretically predicted values by the $\vec{k}\cdot\vec{p}$ method. The calculated $\Delta_0$ splittings are given for reference.

## V. CONCLUSION

The wavelength-modulation derivative spectra of the group-IV and III-V semiconductors, with the ensuing Kramers-Krönig analyses of the dielectric constant line shapes, verify the existence of a hyperbolic exciton interaction in these materials. The interaction occurs at an $M_1$ singularity in all materials studied, except Si, and is located at $\Lambda$ in the Brillouin zone. In InAs, an excitonic interaction at an $M_2$ singularity at 4.7 eV appears to exist.

The location and energy of the interband transitions in these materials agrees with existing band calculations. In particular, the multiplicity of critical point structure expected in the $E_2$ transition region is confirmed. In Si, no excitonic behavior is observed. The interband transitions in Si are dominated by structure from a large region of the Brillouin zone.

---

*Work supported by Army Research Office, Durham, North Carolina.

[1]M. Cardona, *Modulation Spectroscopy* (Academic, New York, 1969).

[2]K. L. Shaklee, J. E. Rowe, and M. Cardona, Phys. Rev. 174, 828 (1968).

[3]J. E. Rowe, F. H. Pollak, and M. Cardona, Phys. Rev. Letters 22, 18 (1969).

[4]A. G. Thompson, J. E. Rowe, and M. Rubenstein, J. Appl. Phys. 40, 8 (1969).

[5]R. R. L. Zucca and Y. R. Shen, Phys. Rev. B 1, 2668 (1970).

[6]R. Braunstein and M. Welkowsky, in *Proceedings of the Tenth International Conference on the Physics of Semiconductors, Cambridge, Mass.*, 1970, edited by S. P. Keller, J. C. Hensel, and F. Stern, (U.S. AEC Division of Technical Information, Springfield, Va., 1970), p. 439.

[7]S. Antoci, E. Reguzzoni, and G. Samoggia, Phys. Rev. Letters 24, 1304 (1970).

[8]B. O. Seraphin and N. Bottka, Phys. Rev. 145, 628 (1966).

[9]M. Cardona, L. Shaklee, and F. H. Pollak, Phys. Rev. 154, 696 (1967).

[10]M. Garfinkel, J. J. Tiemann, and W. E. Engeler, Phys. Rev. 148, 695 (1966).

[11]G. W. Gobeli and E. O. Kane, Phys. Rev. Letters 15, 142 (1965).

[12]B. Batz, Solid State Commun. 4, 241 (1966).

[13]M. Matatagui, A. G. Thompson, and M. Cardona, Phys. Rev. 176, 950 (1968).

[14]C. N. Berglund, J. Appl. Phys. 37, 3019 (1966).

[15]I. Balslev, Phys. Rev. 143, 636 (1966).

[16]R. Braunstein, P. Schreiber, and M. Welkowsky, Solid State Commun. 6, 627 (1968).

[17]J. C. Phillips, Phys. Rev. 136, A1705 (1964).

[18]U. Fano, Phys. Rev. 124, 1866 (1961).

[19]G. F. Koster and J. C. Slater, Phys. Rev. 96, 1208 (1954).

[20]B. Velický and J. Sak, Phys. Status Solidi 16, 147 (1966).

[21]Y. Toyozawa, M. Inoue, T. Inui, M. Okazaki, and E. Hanamura, J. Phys. Soc. Japan Suppl. 21, 133 (1966).

[22]E. O. Kane, Phys. Rev. 180, 852 (1969).

[23]D. T. F. Marple and H. Ehrenreich, Phys. Rev. Letters 8, 87 (1962).

[24]J. Hermanson, Phys. Rev. 166, 893 (1968).

[25]J. D. Walter and M. L. Cohen, Phys. Rev. 183, 763 (1969).

[26]M. L. Cohen and T. K. Bergstresser, Phys. Rev. 141, 789 (1966).

[27]C. W. Higginbotham, F. H. Pollak, and M. Cardona, in *Proceedings of the Ninth International Conference on the Physics of Semiconductors, Moscow* (Nauka, Leningrad, 1968), p. 57.

[28]M. Welkowsky and R. Braunstein, Rev. Sci. Instr. (to be published).

[29]M. Welkowsky, thesis (University of California at Los Angeles, 1971) (unpublished).

[30]D. Brust, Phys. Rev. 134, A1337 (1964).

[31]R. F. Potter, Phys. Rev. 150, 562 (1966).

[32]R. Cahn and M. L. Cohen, Phys. Rev. B 1, 2569 (1970).

[33]L. R. Saravia and D. Brust, Phys. Rev. 176, 915 (1968).

[34]T. M. Donovan, J. E. Fischer, M. Matsuzaki, and W. E. Spicer, Phys. Rev. B 3, 4292 (1971).

[35]D. Brust, Phys. Rev. 139, A489 (1965).

[36]D. J. Stukel and R. N. Euwema, Phys. Rev. B 1, 1635 (1970).

[37]E. O. Kane, Phys. Rev. 146, 558 (1966).

[38]M. L. Cohen and J. C. Phillips, Phys. Rev. 126, 915 (1968).

[39]H. I. Zhang and J. Callaway, Phys. Rev. 181, 1163 (1969).

[40]S. Bloom and T. K. Berstresser, Solid State Commun. 6, 465 (1968).

[41]M. Cardona, J. Appl. Phys. Suppl. 32, 2151 (1961).

[42]T. E. Fischer, Phys. Rev. 139, A1228 (1965).

[43]F. H. Pollak and M. Cardona, Phys. Rev. 142, 530 (1966).